Molecular Psychiatry (2018) 23, 323–334

www.nature.com/mp

ORIGINAL ARTICLE

Translational evaluation of translocator protein as a marker of neuroinflammation in schizophrenia

T Notter[1,2,10], JM Coughlin[3,4,10], T Gschwind[2,5], U Weber-Stadlbauer[1], Y Wang[4], M Kassiou[6,7], AC Vernon[8,9], D Benke[2,5], MG Pomper[3,4], A Sawa[3] and U Meyer[1,2]

Positron emission tomography (PET) imaging with radiotracers that target translocator protein 18 kDa (TSPO) has become a popular approach to assess putative neuroinflammatory processes and associated microglia activation in psychotic illnesses. It remains unclear, however, whether TSPO imaging can accurately capture low-grade inflammatory processes such as those present in schizophrenia and related disorders. Therefore, we evaluated the validity of TSPO as a disease-relevant marker of inflammation using a translational approach, which combined neurodevelopmental and neurodegenerative mouse models with PET imaging in patients with recent-onset schizophrenia and matched controls. Using an infection-mediated neurodevelopmental mouse model, we show that schizophrenia-relevant behavioral abnormalities and increased inflammatory cytokine expression are associated with reduced prefrontal TSPO levels. On the other hand, TSPO was markedly upregulated in a mouse model of acute neurodegeneration and reactive gliosis, which was induced by intrahippocampal injection of kainic acid. In both models, the changes in TSPO levels were not restricted to microglia but emerged in various cell types, including microglia, astrocytes and vascular endothelial cells. Human PET imaging using the second-generation TSPO radiotracer [^{11}C]DPA-713 revealed a strong trend towards reduced TSPO binding in the middle frontal gyrus of patients with recent-onset schizophrenia, who were previously shown to display increased levels of inflammatory cytokines in peripheral and central tissues. Together, our findings challenge the common assumption that central low-grade inflammation in schizophrenia is mirrored by increased TSPO expression or ligand binding. Our study further underscores the need to interpret altered TSPO binding in schizophrenia with caution, especially when measures of TSPO are not complemented with other markers of inflammation. Unless more selective microglial markers are available for PET imaging, quantification of cytokines and other inflammatory biomarkers, along with their molecular signaling pathways, may be more accurate in attempts to characterize inflammatory profiles in schizophrenia and other mental disorders that lack robust reactive gliosis.

Molecular Psychiatry (2018) **23,** 323–334; doi:10.1038/mp.2016.248; published online 17 January 2017

INTRODUCTION

Inflammatory theories in schizophrenia have gained increasing recognition and acceptance in recent years.[1–4] The evidence supporting a role of altered inflammatory processes in the etiology and pathophysiology of schizophrenia involves early-life exposure to infectious pathogens or inflammatory stimuli,[5,6] increased expression of cytokines and other mediators of inflammation in the adult central nervous system (CNS) and periphery,[7–11] as well as signs of glial anomalies.[11–13] Noticeable inflammatory abnormalities, however, may only be present in a subgroup of people with schizophrenia and may predict poorer clinical outcomes and treatment responses.[11,14–17] Additional support for inflammatory theories in schizophrenia stem from clinical trials showing superior beneficial treatment effects in a subset of patients when standard antipsychotic drugs are co-administered with anti-inflammatory compounds, as compared with treatment outcomes using antipsychotic drugs alone.[18–21]

Positron emission tomography (PET) using radiolabeled ligands selective for the 18-kDa translocator protein (TSPO) is one of the most widely used *in vivo* techniques for the assessment of inflammatory abnormalities along the clinical course of schizphrenia.[22–27] Previously known as the peripheral benzodiazepine receptor, TSPO is a transmembrane protein that is located mainly in the outer mitochondrial membrane.[27–29] A wide variety of biological functions have been associated with TSPO, including regulation of cholesterol transport and synthesis of steroid hormones, mitochondrial respiration and ATP production, cell proliferation and apoptosis, and immunomodulation.[28–30] Even though some of the functions of TSPO remain ill-defined,[30] radiotracers against TSPO are widely used to detect putative neuroinflammatory processes and associated microglia activation in schizophrenia.[24–27] The underlying rationale is that TSPO binding increases in response to marked inflammatory stimuli such as acute endotoxemia,[31] which in turn correlates to some

[1]Institute of Pharmacology and Toxicology, University of Zurich-Vetsuisse, Zurich, Switzerland; [2]Neuroscience Center Zurich, University of Zurich and ETH Zurich, Zurich, Switzerland; [3]Department of Psychiatry and Behavioral Sciences, Johns Hopkins Medical Institutions, Baltimore, MD, USA; [4]Russell H. Morgan Department of Radiology and Radiological Science, Johns Hopkins Medical Institutions, Baltimore, MD, USA; [5]Institute of Pharmacology and Toxicology, University of Zurich, Zurich, Switzerland; [6]School of Chemistry, The University of Sydney, Sydney, NSW, Australia; [7]Discipline of Medical Radiation Sciences, The University of Sydney, Sydney, NSW, Australia; [8]MRC Centre for Neurodevelopmental Disorders, King's College London, London, UK and [9]King's College London, Institute of Psychiatry Psychology and Neuroscience, Department of Basic and Clinical Neuroscience, Maurice Wohl Clinical Neuroscience Institute, London, UK. Correspondence: Professor A Sawa, Department of Psychiatry, Johns Hopkins University, 600 North Wolfe Street, Meyer 3-166A, Baltimore, MD 21287, USA or Professor U Meyer, Institute of Pharmacology and Toxicology, University of Zurich-Vetsuisse, Winterthurerstrasse 260, Zurich 8057, Switzerland.
E-mail: asawa1@jhmi.edu or urs.meyer@vetpharm.uzh.ch
[10]These authors contributed equally to the present study.
Received 12 August 2016; revised 14 October 2016; accepted 28 November 2016; published online 17 January 2017

extent with changes in the activation status of microglia.[32] Furthermore, TSPO is robustly increased in neuropathologies that are characterized by marked signs of neuroinflammation, including blood–brain barrier rupture, neurodegeneration and reactive gliosis.[33–35]

Whereas initial studies using first-generation TSPO radiotracers such as [^{11}C]PK11195 have reported increased TSPO binding in patients with schizophrenia,[36,37] studies using second-generation TSPO ligands remain equivocal and provided both positive[38] and negative[39–43] reports. Compared with first-generation TSPO radiotracers, second-generation radiotracers are characterized by increased brain permeability and lower off-target binding such as plasma protein binding, which in turn enhances signal-to-noise ratios.[26,44,45] Notably, a recent within-subject study combining second-generation TSPO PET imaging with peripheral and central cytokine profiling found no clear relationship between low-grade inflammation and TSPO binding in recent-onset schizophrenia.[41] Therefore, it remains unclear whether subtle changes in inflammatory processes, such as those present in schizophrenia, can be accurately captured by TSPO PET imaging.

To advance our understanding of the putative relationship between TSPO and inflammatory alterations in schizophrenia, we implemented a translational approach that combined investigations in a disease-relevant animal model with imaging studies in patients with recent-onset schizophrenia. We used a well-established neurodevelopmental mouse model that has been developed based on the epidemiological evidence linking maternal immune activation (MIA) with increased risk of schizophrenia in the offspring.[5,6,46] In this model, pregnant mice are treated with the viral mimic poly(I:C) (POL; = polyriboinosinic–polyribocytidylic acid), which induces a cytokine-associated viral-like acute-phase response in maternal and fetal compartments.[47,48] Prenatal POL treatment in mice leads to multiple behavioral, cognitive and neuronal disturbances in the adult offspring, many of which are implicated in schizophrenia and related disorders.[46–50] Prenatal POL exposure has also been shown to induce persistent signs of low-grade inflammation in the CNS.[51,52] The MIA model thus offers a unique opportunity to identify possible changes in TSPO expression in a neurodevelopmental animal model with relevance to schizophrenia, and to examine the putative relationship between TSPO and low-grade inflammatory processes. We further compared the MIA model with a mouse model of acute neuronal injury induced by intrahippocampal injection of kainic acid (KA), which is characterized by severe reactive gliosis.[53–57] The KA model thus served as a positive control (CON) for the hypothesis that TSPO expression is increased in the event of increased microglia activation.[24–27] Based on the findings from the MIA model, we then analyzed PET TSPO binding in selected brain regions of patients with recent-onset schizophrenia and matched CONs. Our human cohort was previously characterized in terms of peripheral and central inflammation, which confirmed a significant elevation of inflammatory cytokines in plasma and cerebrospinal fluid in schizophrenia patients.[41] Thus, we believe the present study provides the first translational evaluation of TSPO as a marker of aberrant inflammatory processes in the context of schizophrenia and related neurodevelopmental disorders.

MATERIALS AND METHODS

Animals

All mouse models (see below) were performed using C57Bl6/N mice (Charles Rivers, Sulzfeld, Germany). All procedures involving animal experimentation had been previously approved by the Cantonal Veterinarian's Office of Zurich, and all efforts were made to minimize the number of animals used and their suffering.

MIA model

Female mice were subjected to a timed mating procedure as established previously.[48,50] Pregnant dams were subjected to either a single injection of POL (potassium salt; Sigma–Aldrich, Buchs, St Gallen, Switzerland) or vehicle on gestation day 9 (Supplementary Information). POL (5 mg kg^{-1}) was dissolved in sterile pyrogen-free 0.9% NaCl (vehicle) solution to yield a final concentration of 1 mg ml^{-1} and was administered intravenously into the tail vein (Supplementary Information).

The allocation and housing of POL-exposed and CON offspring are described in the Supplementary Information. Three independent cohorts of CON and POL offspring were used, each stemming from multiple independent litters to avoid litter effects (Supplementary Information). Cohorts 1 and 2 were first subjected to behavioral testing to allow correlative analyses between behavioral and immunohistochemical readouts (see below). Offspring in cohort 3 were assigned to *ex vivo* TSPO ligand-binding studies and cytokine measurements (see below) without prior behavioral testing.

Behavioral testing in the MIA model

Male and female POL and CON offspring were tested in paradigms of prepulse inhibition (PPI) of the acoustic startle reflex (cohort 1) and social interaction (cohort 2) to confirm the presence of selected schizophrenia-relevant behavioral phenotypes.[50,58–60] A detailed description of the test apparatuses and procedures is provided in the Supplementary Information. Behavioral testing was conducted when the offspring reached 12 weeks of age based on previous findings.[50,52,61,62]

KA injection model

The KA model followed procedures established and validated before.[54] As described in the Supplementary Information, KA was injected unilaterally into the CA1 region of the right dorsal hippocampus, and the animals ($N = 8$) were killed for immunohistochemical investigations of TSPO and glial markers 3 weeks post injection (Supplementary Information). The post-injection interval was selected based on previous studies showing marked reactive gliosis in response to KA injection at this interval.[54–57]

Immunohistochemistry in animal models

CON and POL mice were perfused intracardially with 4% phosphate-buffered paraformaldehyde (PFA) solution containing 15% picric acid, followed by post-fixation in PFA, antigen retrieval and cryoprotection (Supplementary Information). Animals with intrahippocampal KA or vehicle injections were perfused intracardially with oxygenated artificial cerebrospinal fluid, followed by post-fixation in PFA and cryoprotection as previously described.[63] The brain samples were cut coronally with a sliding microtome at 30 μm (MIA model; 8 serial sections) or 40 μm (KA model; 12 serial sections) and stored at − 20 °C in antifreeze solution (Supplementary Information).

Immunoperoxidase (IP) staining was used to visualize and quantify TSPO, microglia and astrocytes (Supplementary Information). Immunofluorescence (IF) staining was used to quantify the levels of TSPO protein within microglia, astrocytes or vascular endothelial cells (Supplementary Information). Primary and secondary antibodies used in IP and IF procedures are summarized in Supplementary Table 1.

Microscopy and optical densitometry in animal models

Images of IP-stained sections were acquired with a digital camera using bright-field illumination (Zeiss Axioskop, Zeiss, Jena, Germany), whereas images of triple IF-stained sections were acquired using confocal laser scanning microscopy (LSM-700; Zeiss; Supplementary Information). Quantification of total TSPO, CD68 and GFAP in IP-stained sections was achieved by means of optical densitometry using NIH ImageJ software (https://imagej.nih.gov/ij/) (Supplementary Information) and was performed using male and female CON and POL offspring to reveal possible sex-dependent effects, and in adult males subjected to intrahippocampal KA injections. The total number of Iba^{+} microglia cells was quantified in male CON and POL offspring using unbiased stereological estimations (Supplementary Information); and microglia cell morphology (cell soma size and number of primary branches) were assessed on IP-stained Iba1 sections according to methods established before[52] and described in the Supplementary Information.

For IF-stained sections, total TSPO intensity and TSPO intensity co-localized with microglia (Iba1 or CD68), astrocytes (GFAP) or vascular

endothelial cells (Glut1) were measured and calculated on *z*-projected image stacks using a customized macro for the ImageJ software (Supplementary Information). Based on the lack of sex-dependent effects in the analyses of IP-stained sections, IF-stained sections in the MIA model were analyzed in male offspring only.

Images were acquired on consecutive serial sections and analyzed in the medial prefrontal cortex (mPFC), CA1–CA3 regions (CA) of the hippocampus and dentate gyrus. These brain regions were selected based on their relevance to schizophrenia.[64,65]

TSPO autoradiography in the MIA model

Ex vivo TSPO ligand-binding studies were performed in the mPFC of CON and POL offspring using autoradiography.[66] Animals (12 weeks of age; $N = 9$ per group) were killed by decapitation. Their brains were immediately removed on an ice-chilled plate, divided into left and right hemispheres, frozen with powdered dry ice, and stored at −80 °C until further processing. Autoradiography was performed on the right brain hemisphere, whereas the left hemisphere was used for the quantification of inflammatory cytokines in the mPFC (see below). TSPO ligand binding was assessed using the first-generation radiotracer [^{3}H]PK11195 and the second-generation TSPO radiotracer [^{3}H]DPA-713 (Supplementary Information). The former was selected because it represents the prototypical first-generation TSPO radiotracer,[26,28] whereas the latter was chosen to match the TSPO PET imaging study in patients with recent-onset schizophrenia and CON subjects (see below).

Quantification of inflammatory cytokines in the MIA model

Protein levels of interleukin (IL)-1β, IL-5, IL-6, IL-10, tumor necrosis factor-α and interferon-γ were quantified in plasma and in the left-hemisphere mPFC of CON and POL offspring ($N = 9$ per group) using a customized Meso-Scale Discovery V-Plex electrochemiluminescence assay for mice, which allows ultralow detection of multiple cytokines.[67] The quantification of cytokines followed procedures validated before[52] and is described in the Supplementary Information.

Human subjects

The PET imaging data set included in this study consisted of data from 12 patients with recent onset of schizophrenia and 14 healthy CON subjects (Supplementary Information). The cohort used here is identical to the patients and CONs with PET imaging data included in a recent study.[41] The average duration of disease among patients was 2.1 ± 1.4 years. Antipsychotic medication use by the patients was reported in chlorpromazine equivalents and ranged from 0 to 1119 (mean 494.8 ± 382.0). The PET imaging study was approved by the Johns Hopkins Institutional Review Board, and all participants provided written informed consent.

PET in patients with schizophrenia and CONs

PET imaging was conducted using the second-generation TSPO radiotracer [^{11}C]DPA-713. [^{11}C]DPA-713 was selected because it is characterized by an increased signal-to-noise ratio as compared with the first-generation radiotracer [^{11}C]PK11195.[44,45,68] Like other second-generation TSPO radiotracers, [^{11}C]DPA-713 differentially binds to TSPO depending on the single-nucleotide polymorphism (SNP), rs6971, in exon 4 of the TSPO gene, which results in an alanine to threonine substitution.[69,70] Based on genotyping of the rs6971 SNP, each individual undergoing a [^{11}C]DPA-713 PET scan can therefore be grouped as either high (C/C genotype)-, mixed (C/T genotype)- or low (T/T genotype)-affinity binders.[70] As fully described before,[41] each individual included in our clinical setting was genotyped with respect to the rs6971 SNP. Among the 26 participants, genotyping of the rs6971 polymorphism within the TSPO gene revealed 17 individuals with C/C genotype and 9 participants with C/T genotype.[41]

PET images were acquired on High Resolution Research Tomograph scanner (Siemens Healthcare, Knoxville, TN, USA) after a bolus injection of 684.0 ± 53.1 MBq of [^{11}C]DPA-713 and were processed and analyzed as described in the Supplementary Information. Based on the findings provided by the MIA model, [^{11}C]DPA-713 binding was analyzed in the middle frontal gyrus (MFG). The MFG spans a substantial part of the human dorsolateral prefrontal cortex,[71,72] which in turn is structurally and functionally related to the mPFC in rodents.[73,74] The primary PET-based regional binding outcome was total distribution volume (V_T),[75] which was calculated using the Logan method (Supplementary Information).

Statistical analysis

All data met the assumptions of normal distribution and equality of variance. All mouse model data were analyzed using analysis of variance (ANOVA), multivariate analysis of variance, independent Student's *t*-tests (two-tailed) and Pearson's product moment correlations as described in the Supplementary Information. These analyses were conducted using SPSS Statistics (version 22.0, IBM, Armonk, NY, USA) and Prism (version 5.0; GraphPad Software, La Jolla, CA, USA). Exclusion of animals was not applied.

The primary PET outcome measure (V_T) was analyzed using multivariate general linear modeling using SPSS Statistics (Version 22.0, IBM). The V_T values obtained from the MFG were modeled based on the relationship to between-subject factors, including cohort (patients, CONs) and TSPO genotype (C/C: high-affinity binder, C/T: mixed-affinity binder) as independent fixed factors. Hence, the PET imaging data were analyzed using a 2 × 2 (cohort (patients, CONs) × TSPO genotype (C/C, C/T)) analysis of variance to account for the expected genotype effect on TSPO binding.[70]

Statistical significance was set at $P < 0.05$ for all analyses.

RESULTS

Lower prefrontal TSPO density in a mouse model relevant to schizophrenia

We evaluated TSPO protein density in the mouse MIA model, which was previously shown to capture a multitude of brain and behavioral abnormalities relevant to schizophrenia.[46–50] Here we confirm that adult offspring exposed to MIA show behavioral abnormalities implicated in schizophrenia, namely, impaired PPI of the acoustic startle reflex[50,61,62] (Figure 1a; Supplementary Figures 1a and b) and reduced social interaction[62,76,77] (Figure 1b; Supplementary Figure 1c). The effects of MIA on PPI and social interaction were independent of sex and similarly emerged in male and female offspring (Supplementary Figure 2).

We used IP staining to visualize and measure TSPO levels in distinct brain areas relevant to schizophrenia, including the mPFC, CA and dentate gyrus regions (Figure 1d). TSPO immunoreactivity was clearly present in various cell types, including cells displaying varying degrees of ramification and cells of the brain vasculature (Figure 1c). Prenatal immune activation decreased TSPO density in the mPFC but not in CA or dentate gyrus regions (Figure 1e). The MIA-induced reduction in prefrontal TSPO density emerged in both males and females (Supplementary Figure 3) and was confirmed in two independent cohorts of offspring (Figures 1e and f). Prefrontal TSPO density correlated positively with PPI scores in offspring exposed to MIA but not in CON offspring (Figure 1g). There was no correlation between TSPO density and social interaction scores (Figure 1h).

Cellular sources of lower prefrontal TSPO density in a mouse model relevant to schizophrenia

Using the MIA model, we further performed triple IF staining to measure the intensity of TSPO co-localized with Iba1$^+$ microglia, GFAP$^+$ astrocytes and Glut1$^+$ vascular endothelial cells. 4,6-Diamidine-2-phenylindole dihydrochloride (DAPI) was used as nuclear counterstain in all IF preparations. Based on the preceding results (Figures 1e and f), we focused the co-localization studies on prefrontal sections obtained from MIA-exposed and CON offspring.

We identified clear co-localization between TSPO and all cell types investigated (Figures 2a, c and e). Hence, the analyses of IF-stained sections confirmed the impressions obtained from the initial IP staining, which suggested widespread TSPO protein expression in multiple CNS cell types (Figure 1c). In agreement with the results obtained using IP staining (Figures 1e and f), total TSPO intensity was consistently reduced in IF-stained sections of MIA-exposed offspring relative to CONs (Figures 2b, d and f). Most interestingly, the analyses of co-localization demonstrated that the MIA-induced reduction in TSPO intensity was similarly present in

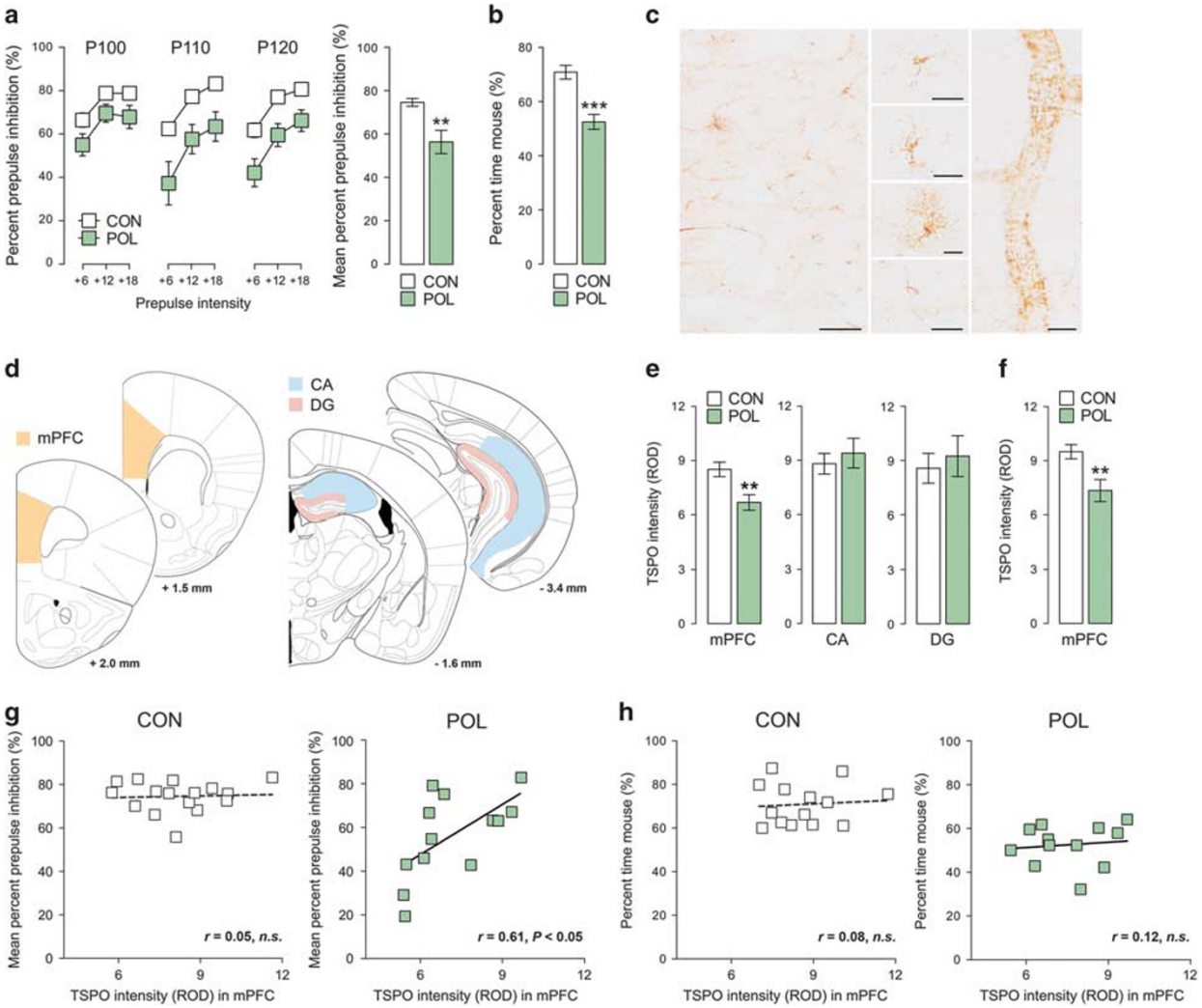

Figure 1. Behavioral phenotypes and brain translocator protein (TSPO) levels in adult offspring exposed to prenatal poly(I:C)-induced immune activation (POL) or control (CON) treatment. (**a**) Prepulse inhibition of the acoustic startle reflex. The line plot shows percent prepulse inhibition as a function of different pulse intensities (P-100, P-110 and P-120, corresponding to 110, 110 and 120 dB_A) and prepulse intensities (+6, +12 and +18 dB_A above background of 65 dB_A); the bar plot depicts the mean prepulse inhibition scores across all pulse and prepulse conditions. $^{**}P < 0.01$, reflecting the main effect of prenatal treatment ($F_{(1,25)} = 11.36$) based on $2 \times 2 \times 3 \times 3$ (prenatal treatment × sex × prepulse level × pulse level) analysis of variance (ANOVA); *N*(CON) = 16 (8 m, 8 f), *N*(POL) = 13 (6 m, 7 f). (**b**) Social interaction test, in which offspring were allowed to concomitantly explore an inanimate dummy object and an unfamiliar live mouse. The bar plot shows the percent time spent with an unfamiliar mouse. $^{***}P < 0.001$, reflecting the main effect of prenatal treatment ($F_{(1,22)} = 25.26$) based on 2×2 (prenatal treatment × sex) ANOVA; *N*(CON) = 14 (6 m, 8 f), *N*(POL) = 12 (5 m, 7 f). (**c**) Representative TSPO immunoperoxidase-stained mouse brain sections. TSPO is expressed in various cell types, including cells displaying varying degrees of ramification and cells of the brain vasculature. Scale bars, 100 μm (left photomicrograph); 30 μm (middle and right photomicrographs). (**d**) Schematic coronal brain sections delineating the prefrontal and hippocampal areas investigated with reference to bregma. TSPO immunoreactivity in the medial prefrontal cortex (mPFC; highlighted in yellow) was assessed in sections ranging from bregma +2.0 to +1.5 mm and included anterior cingulated, prelimbic and infralimbic subregions; hippocampal TSPO immunoreactivity was measured in the CA1–CA3 regions (CA; highlighted in light blue) and in the dentate gyrus (DG; highlighted in salmon) ranging from bregma − 1.6 to − 3.4 mm. (**e**) TSPO intensity (relative optical density, ROD) in the mPFC, CA and DG regions. $^{**}P < 0.01$, reflecting the main effect of prenatal treatment ($F_{(1,25)} = 11.84$) based on 2×2 (prenatal treatment × sex) ANOVA; *N*(CON) = 16 (8 m, 8 f), *N*(POL) = 13 (6 m, 7 f). (**f**) Replication of reduced TSPO intensity (ROD) in the mPFC of POL offspring using an independent cohort. $^{**}P < 0.01$, reflecting the main effect of prenatal treatment ($F_{(1,22)} = 8.47$) based on 2×2 (prenatal treatment × sex) ANOVA; *N*(CON) = 14 (6 m, 8 f), *N*(POL) = 12 (5 m, 7 f). (**g**) Pearson's product moment correlations between sensorimotor gating (indexed by the mean percent prepulse inhibition) and prefrontal TSPO intensity in CON (*N* = 16) and POL (*N* = 13) offspring. (**h**) Pearson's product moment correlations between social approach behavior (indexed by the percent time spent with an unfamiliar mouse) and prefrontal TSPO intensity in CON (*N* = 14) and POL (*N* = 12) offspring. All values expect correlations are means ± s.e.m.

microglia (Figure 2b), astrocytes (Figure 2d) and vascular endothelial cells (Figure 2f). $Iba1^+$, $GFAP^+$ and $Glu1^+$ area fractions did not differ between groups (Figures 2b, d and f), suggesting that MIA reduces prefrontal TSPO intensity without inducing overt glial or vascular cell changes *per se*.

Prefrontal neuroimmune profiles in a mouse model relevant to schizophrenia

The analyses of $Iba1^+$ and $GFAP^+$ area fractions in IF-stained sections indicated that MIA did not cause overt microglial or astroglial anomalies in the mPFC (Figures 2b and d). To further

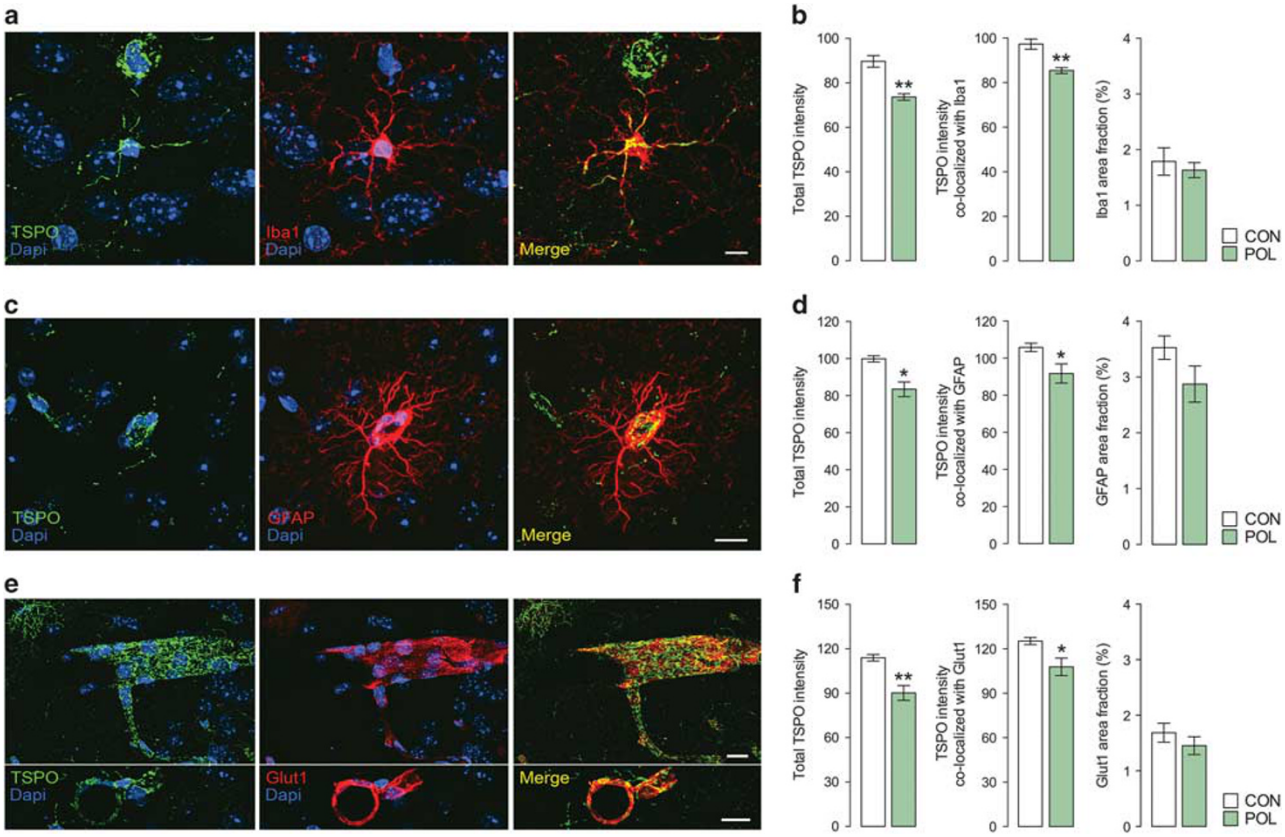

Figure 2. Cellular localization of translocator protein (TSPO) expression in the medial prefrontal cortex of adult offspring exposed to prenatal poly(I:C)-induced immune activation (POL) or control (CON) treatment. (**a**) Triple immunofluorescence image showing nuclear staining (DAPI, blue), microglia (Iba1, red) and TSPO (green). Co-localization between TSPO and Iba1 appears yellow in the merged image. (**b**) Total TSPO intensity (optical density, OD), TSPO intensity (OD) co-localized with Iba1-positive microglia and area fraction (%) of Iba1-positive staining. (**c**) Triple immunofluorescence image showing nuclear staining (DAPI, blue), astrocytes (GFAP, red) and TSPO (green). Co-localization between TSPO and GFAP appears yellow in the merged image. (**d**) Total TSPO intensity (OD), TSPO intensity (OD) co-localized with GFAP-positive astrocytes and area fraction (%) of GFAP-positive staining. (**e**) Triple immunofluorescence image showing nuclear staining (DAPI, blue), brain vasculature (Glut1, red) and TSPO (green). Co-localization between TSPO and Glut1 appears yellow in the merged image. (**f**) Total TSPO intensity (OD), TSPO intensity (OD) co-localized with Glut1-positive brain vasculature and area fraction (%) of Glut1-positive staining. $^{*}P < 0.05$ and $^{**}P < 0.01$, based on *t*-tests (two-tailed); $N(\mathrm{CON}) = 8$ and $N(\mathrm{POL}) = 6$. All values are means ± s.e.m. All images represent stacks of eight pictures spaced 1 μm; scale bars in all images, 10 μm.

examine this hypothesis, we assessed Iba1, CD68 and GFAP immunoreactivity on IP-stained prefrontal sections. Unbiased stereological estimations of $Iba1^{+}$ microglia showed that MIA did not alter the density (number of immunoreactive cells per mm^3) of total microglia in the mPFC (Figure 3a). There were also no group differences with respect to cell soma area and primary branches of $Iba1^{+}$-positive cells (Figure 3a), suggesting that activation-related morphology of prefrontal microglia was not changed by MIA. Consistent with previous investigations[51,52] and with our analyses of IF-stained sections (Figures 2b and d), there were also no group differences with regards to prefrontal CD68 (Figure 3b) and GFAP (Figure 3c) relative optical densities in the mPFC. MIA-exposed offspring displayed, however, significantly increased prefrontal protein levels of several inflammatory cytokines, including IL-1β, IL-5 and IL-6, and a trend towards elevated prefrontal interferon-γ protein (Figure 3d). Contrary to the mPFC, plasma cytokines were either unchanged or decreased in MIA-exposed offspring relative to CONs (Supplementary Figure 4). Our results thus show that MIA induces selective neuroimmune changes that are characterized by increased inflammatory cytokine expression in the absence of overt micro-/astroglial anomalies or signs of systemic inflammation.

TSPO ligand binding in patients with recent-onset schizophrenia

We aimed at translating the preclinical findings of altered prefrontal TSPO expression to the human clinical condition. To this end, we analyzed PET TSPO binding in the MFG of patients with recent-onset schizophrenia and matched CON subjects using the second-generation TSPO radiotracer, [^{11}C]DPA-713. Consistent with previous studies,[70,78] high-affinity binders harboring the C/C TSPO genotype generally displayed higher V_T values for [^{11}C]DPA-713 compared with mixed-affinity binders with the C/T genotype (Figure 4a). There was a strong trend towards reduced [^{11}C]DPA-713 binding in the MFG of patients with recent-onset schizophrenia relative to CON subjects independently of the TSPO genotype (Figure 4a). Quantitative analysis of the magnetic resonance imaging-based segmentation of the MFG showed no significant evidence of changes in MFG volume in patients with recent onset of schizophrenia ($39.19 \pm 6.75\ cm^3$) compared with CONs ($42.73 \pm 4.06\ cm^3$). There was also no significant difference in intracranial volume between patients and CONs as previously reported.[41]

We complemented the human *in vivo* PET imaging studies with *ex vivo* autoradiography experiments assessing TSPO ligand binding in the mPFC of MIA-exposed and CON offspring. There were no significant group differences in *ex vivo*

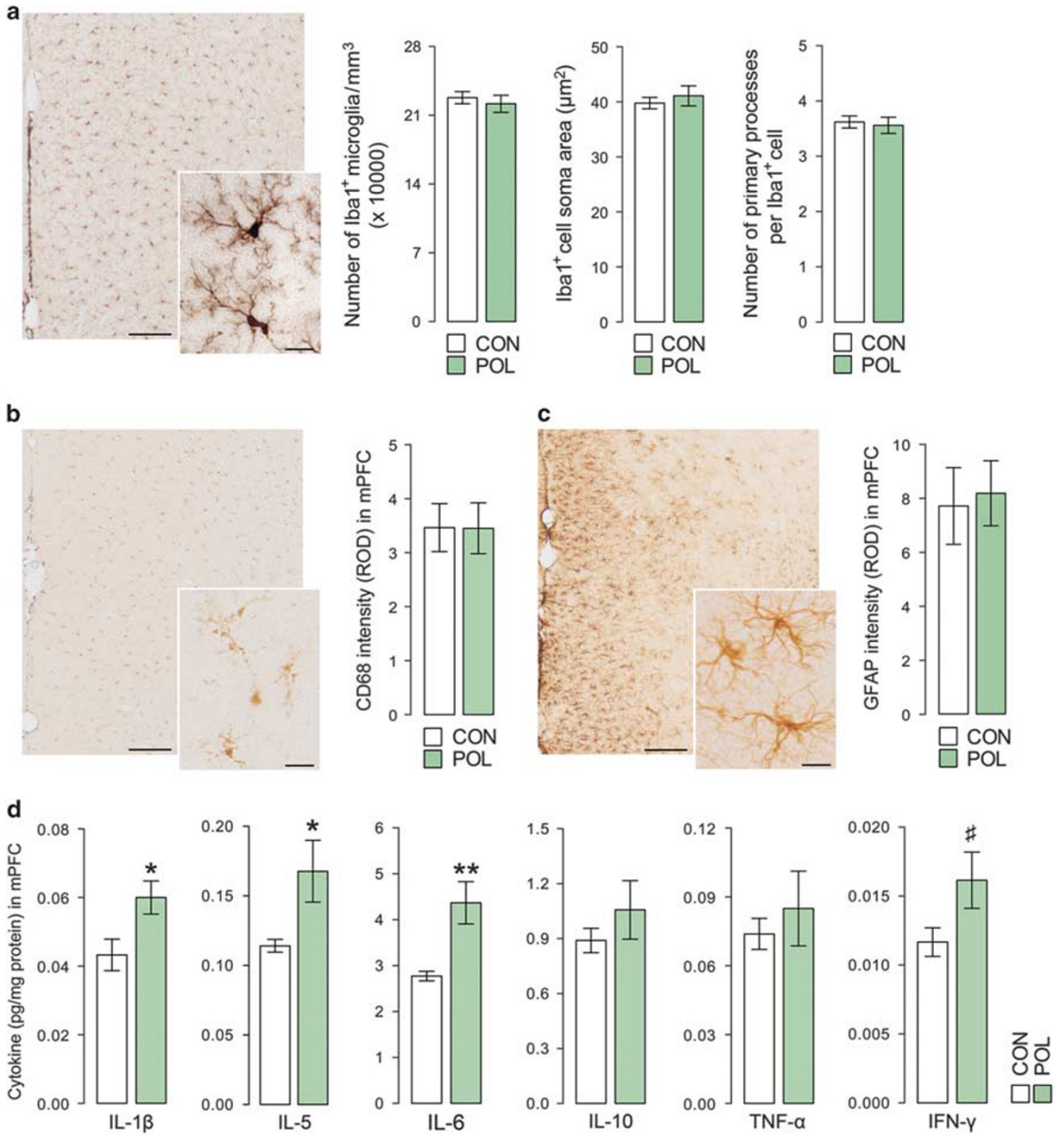

Figure 3. Inflammatory phenotypes in adult offspring exposed to prenatal poly(I:C)-induced immune activation (POL) or control (CON) treatment. (**a**) The photomicrograph depicts Iba1-immunoreactive microglia in the medial prefrontal cortex (mPFC); scale bars, 300 µm (low magnification); 25 µm (high magnification). The bar plots show stereological estimates of Iba1$^+$ microglia (cells per mm^3), soma size of Iba1$^+$ microglia and number of primary processes of Iba1$^+$ microglia in the mPFC of CON and POL offspring. *N*(CON) = 16, *N*(POL) = 13. (**b**) The photomicrograph depicts CD68-immunoreactive microglia in the mPFC; scale bars, 300 µm (low magnification) and 25 µm (high magnification). The bar plot shows CD68 intensity (relative optical density, ROD) in the mPFC of CON and POL offspring. *N*(CON) = 16, *N*(POL) = 13. (**c**) The photomicrograph depicts GFAP-immunoreactive astrocytes in the mPFC; scale bars, 300 µm (low magnification) and 25 µm (high magnification). The bar plot shows GFAP intensity (ROD) in the mPFC of CON and POL offspring. *N*(CON) = 16, *N*(POL) = 13. (**d**) Cytokine protein levels (pg mg^{-1} total protein) in the mPFC of CON and POL offspring. $^*P < 0.05$, $^{**}P < 0.01$ and $^{\sharp}P = 0.067$, based on *t*-tests following a significant prenatal treatment effect in multivariate analysis of variance (Wilks's $\Lambda = 0.351$, $F_{(6,11)} = 4.62$, $P < 0.05$). *N*(CON) = 9, *N*(POL) = 9. All values are means ± s.e.m.

autoradiography, neither when using the first-generation TSPO radiotracer [^{3}H]PK11195 (Figure 4b) nor when using the second-generation radiotracer [^{3}H]DPA-713 (Figure 4c). Moreover, there were no significant correlations between *ex vivo* [^{3}H]PK11195 or [^{3}H]DPA-713 binding and inflammatory cytokines in the mPFC or plasma of MIA-exposed or CON offspring (Supplementary Table 2).

Increased TSPO density in a mouse model of neurodegeneration and reactive gliosis

In a last series of experiments, we explored TSPO expression in the KA mouse model of acute neurodegeneration and reactive gliosis. Consistent with previous findings,[54–57] we found that intrahippocampal KA injection induced clear signs of reactive gliosis, as evident by the marked increases in microglial CD68 and astroglial

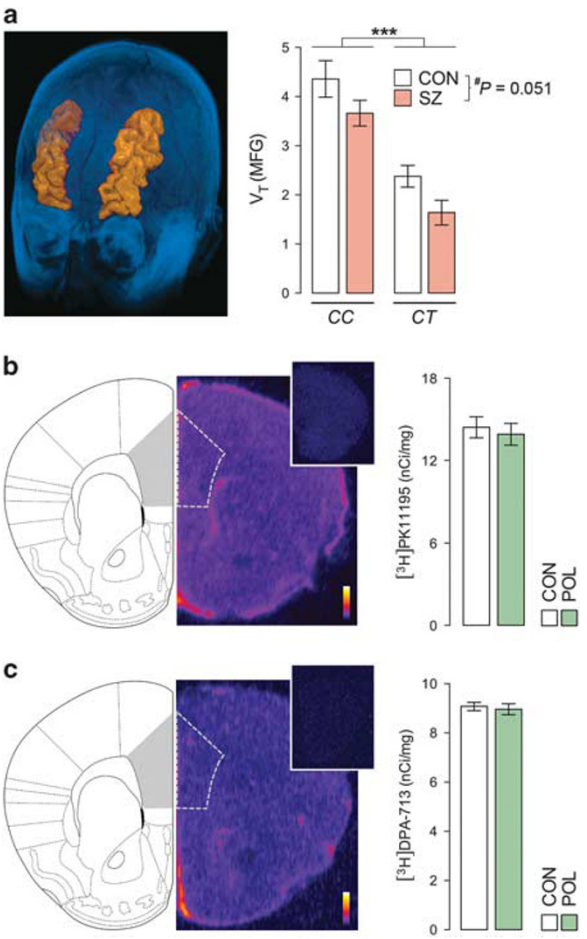

Figure 4. Translocator protein (TSPO) ligand binding in schizophrenia (SZ) and the maternal immune activation model. (**a**) The illustration displays a three-dimensional view of a representative magnetic resonance image demonstrating the middle frontal gyrus (MFG; highlighted in orange), which was selected as the primary region of interest in the human positron emission tomography imaging with [^{11}C]DPA-713. The bar plot shows [^{11}C]DPA-713 distribution volumes (V_T) in the MFG of patients with recent-onset SZ and matched control subjects (CON). High- and mixed-affinity binders harboring the C/C and C/T TSPO genotypes, respectively, are depicted separately. ***$P < 0.001$, reflecting the main effect of TSPO genotype (C/C versus C/T genotype); and $^{\#}P = 0.051$, reflecting the main effect of cohort (CON versus SZ) at statistical trend level, based on 2 × 2 (cohort (SZ patients, CONs) × TSPO genotype (C/C, C/T)) analysis of variance. *N*(CON, C/C) = 9, *N*(CON, C/T) = 5, *N*(SZ, C/C) = 8; *N*(SZ, C/T) = 4. (**b**) *Ex vivo* autoradiography using the first-generation TSPO radiotracer [^{3}H]PK11195 in adult offspring exposed to prenatal poly(I:C)-induced immune activation (POL) or CON treatment. Schematic representation and representative binding pattern in the prefrontal region of interest are outlined in gray (schematic illustration) and highlighted by the dashed line in the color-coded image. The insert represents non-specific binding as assessed by a competitive displacement binding assay using Ro5-4864. The bar plot shows the quantification of [^{3}H]PK11195 binding (nCi/mg) in CON (*N* = 9) and POL (*N* = 9) offspring. (**c**) *Ex vivo* autoradiography using the second-generation TSPO radiotracer [^{3}H]DPA-713 in adult CON and POL offspring. Schematic representation and representative binding pattern in the region of interest are outlined in gray (schematic illustration) and highlighted by the dashed line in the color-coded image. The insert represents non-specific binding as assessed by a competitive displacement binding assay using Ro5-4864. The bar plot shows the quantification of [^{3}H]DPA-713 binding (nCi mg^{-1}) in CON (*N* = 9) and POL (*N* = 9) offspring. All values are means ± s.e.m.

GFAP expression in IP-stained sections (Figures 5a and b). Notably, these glial changes were accompanied by a robust increase in TSPO IP immunoreactivity (Figure 5c).

IF staining coupled with confocal laser scanning microscopy further demonstrated that the KA-induced increase in TSPO expression similarly emerged in CD68$^+$ microglia (Figure 5d), GFAP$^+$ astrocytes (Figure 5e) and Glut1$^+$ vascular endothelial cells (Figure 5f). Together, these results show that multiple cells of the CNS increase TSPO expression in the event of acute neurodegeneration and reactive gliosis.

DISCUSSION

PET imaging using TSPO radiotracers has become a popular approach to assess central inflammatory abnormalities in schizophrenia and related neurodevelopmental disorders.[22–25] These investigations have been largely motivated by findings showing increased TSPO binding occurring in response to pronounced inflammatory stimuli such as acute endotoxemia[31,32] or in the event of neurodegeneration and reactive gliosis.[33–35] Using a mouse model of acute neurodegeneration induced by intrahippocampal KA injection, our study confirms that TSPO is markedly upregulated in the event of reactive gliosis. Such severe neuroinflammatory conditions, however, critically differ from the neuroimmune profiles of most neurodevelopmental disorders such as schizophrenia.[9–14] To mimic the latter, we used a well-characterized mouse model that is based on MIA-induced neurodevelopmental disruption.[46–50] Consistent with previous findings,[50–52,61,62] adult mice exposed to POL-induced MIA displayed schizophrenia-relevant behavioral abnormalities and elevated prefrontal levels of inflammatory cytokines in the absence of overt glial anomalies. Although the precise sources of increased prefrontal cytokine expression remain elusive (Supplementary Discussion), the neuroimmune profile in the MIA model is reminiscent of cytokine-associated inflammatory abnormalities present in prefrontal areas of (a subset of) chronic patients with schizophrenia.[10,11]

Our findings challenge the widely accepted assumption that increased TSPO expression in schizophrenia generally mirrors central inflammation and altered microglia activity.[23,36–40] First, the MIA-based neurodevelopmental disruption model shows that increased levels of inflammatory cytokines can emerge concomitantly with a downregulation (rather than upregulation) of TSPO. Second, the downregulation of prefrontal TSPO in the MIA model was not associated with overt signs of microglial anomalies nor was there an association between microglia morphology and TSPO expression in this neurodevelopmental animal model relevant to schizophrenia. Consistent with previous immunohistochemical studies in the rodent and human brain,[79,80] we found that TSPO immunoreactivity was clearly present in various CNS cell types, including microglia, astrocytes and vascular endothelial cells. Moreover, the MIA and KA models both revealed altered TSPO levels in all these cell types. These findings thus emphasize that altered TSPO expression or ligand binding cannot be equated with altered microglia activity only, even in neuropathologies that involve severe microgliosis. Third, a strong trend towards reduced TSPO ligand binding was also observed in PET imaging of recent-onset schizophrenia relative to CONs. It is important to point out that our cohort of patients and CONs were previously characterized in terms of inflammatory profiles at the time the PET scans were acquired.[41] These previous investigations confirmed a significant elevation of inflammatory cytokines in the cerebrospinal fluid and plasma of patients relative to CONs.[41] In this previous study, the interval between blood sample collection and the initiation of the PET scan was < 1 h,[41] which allowed us to explore possible correlations between TSPO binding and cytokine levels in close temporal proximity. These latter analyses, however, did not reveal significant correlations between peripheral (or

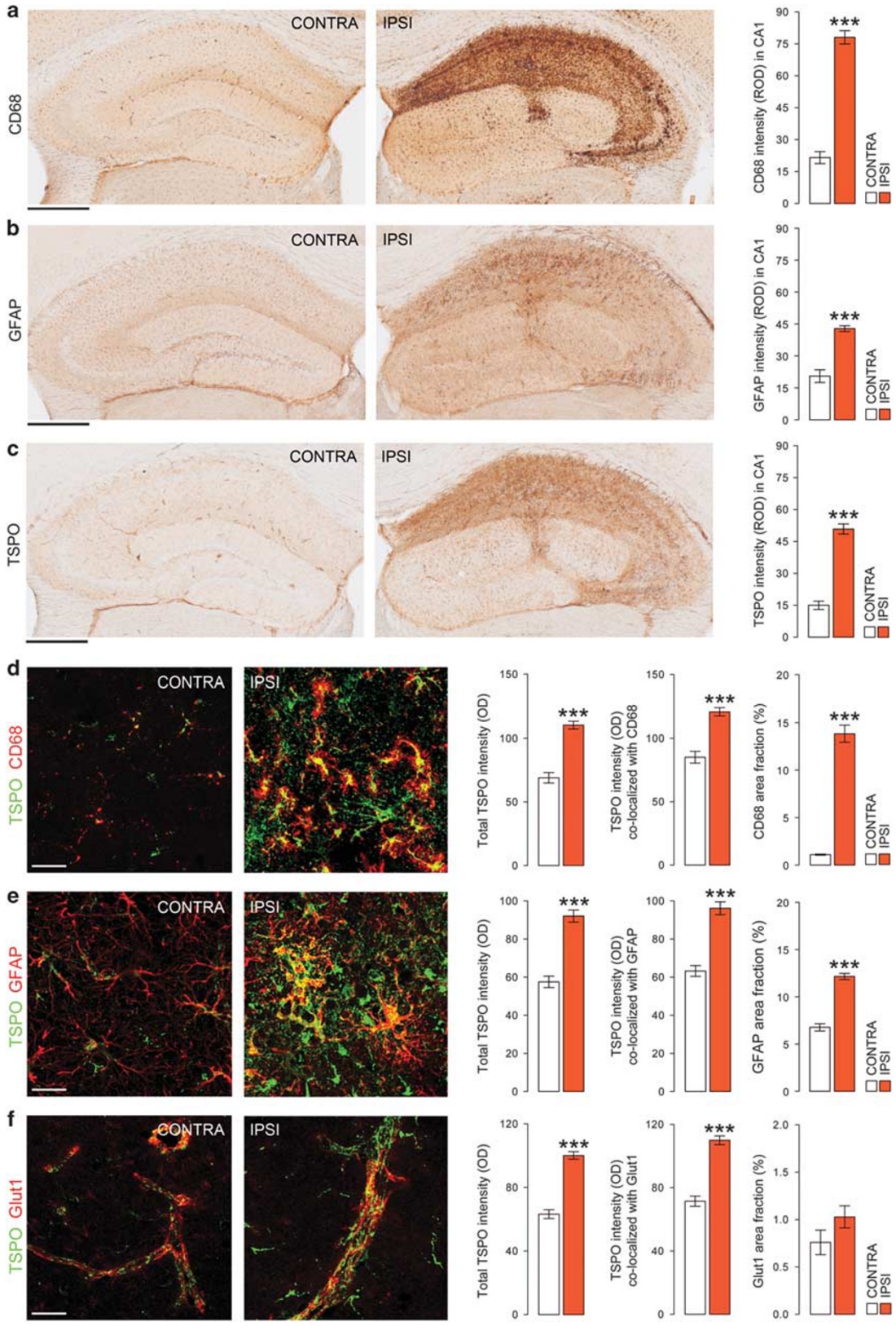

cerebrospinal fluid) cytokine contents and TSPO binding in patients with recent-onset schizophrenia relative or CONs.[41] Consistent with these clinical data, the current MIA model did not provide evidence for the hypothesis that TSPO binding correlates with elevated cytokine expression in prefrontal areas, neither for first-generation ([^{3}H]PK11195) nor for second-generation ([^{3}H]DPA-713) TSPO radiotracers. Taken together, our translational study strongly suggests that there is no positive relationship between TSPO expression and central low-grade inflammation in schizophrenia. If anything, this relationship tends

Figure 5. Glial responses and translocator protein (TSPO) expression after intrahippocampal kainic acid injection. Kainic acid was injected unilaterally (IPSI) into the CA1 region of adult male C57BL6 mice; the contralateral side (CONTRA) served as control. (**a**) The photomicrographs depict representative images of immunoperoxidase-stained brain sections against CD68. The bar plot shows CD68 intensity (relative optical density, ROD) in the CA1 region of the CONTRA and IPSI sides. (**b**) The photomicrographs depict representative images of immunoperoxidase-stained brain sections against GFAP. The bar plot shows GFAP intensity (ROD) in the CA1 region of the CONTRA and IPSI sides. (**c**) The photomicrographs depict representative images of immunoperoxidase-stained brain sections against TSPO. The bar plot shows TSPO intensity (ROD) in the CA1 region of the CONTRA and IPSI sides. (**d**) Merged double-immunofluorescence staining for TSPO (green) and CD68 (red) in CONTRA and IPSI CA1 sides. Co-localization between TSPO and CD68 appears yellow. Bar plots represent total TSPO intensity (optical density, OD), TSPO intensity (OD) co-localized with CD68-positive microglia and area fraction (%) of CD68-positive staining. (**e**) Merged double-immunofluorescence staining for TSPO (green) and GFAP (red) in CONTRA and IPSI CA1 sides. Co-localization between TSPO and GFAP appears yellow. Bar plots represent total TSPO intensity (OD), TSPO intensity (OD) co-localized with GFAP-positive astrocytes and area fraction (%) of GFAP-positive staining. (**f**) Merged double-immunofluorescence staining for TSPO (green) and Glut1 (red) in CONTRA and IPSI CA1 sides. Co-localization between TSPO and Glut1 appears yellow. Bar plots represent total TSPO intensity (OD), TSPO intensity (OD) co-localized with Glut1-positive brain vasculature and area fraction (%) of Glut1-positive staining. $^{***}P < 0.001$, based on *t*-tests (two-tailed) and $N = 8$ for all data; all values are means ± s.e.m. Images in (**d**–**f**) represent stacks of eight pictures spaced 0.45 μm. Scale bars, 800 μm (**a**–**c**); 20 μm (**d**–**f**).

to be negative and is unlikely driven by sole changes in microglia activity.

A negative relationship between central low-grade inflammation and TSPO expression may be explained by the known anti-inflammatory properties of TSPO.[81–85] In this regard, upregulation of TSPO may be an adaptive response mechanism that counteracts or limits acute inflammatory responses in the CNS, whereas a downregulation may facilitate chronic low-grade inflammatory processes. Under certain pathological conditions, however, changes in TSPO may not be primarily triggered by inflammatory factors such as cytokines, but rather by other pathophysiological mechanisms. Such alternative mechanism may include changes in cellular metabolism, mitochondrial dysfunctions and/or oxidative stress,[86–89] all of which have been implicated in schizophrenia[4,90,91] and disease-relevant animal models.[92–94]

Whatever processes involved, our findings suggest that a downregulation of TSPO may have a pathological relevance for certain schizophrenia-related behavioral anomalies. In the MIA model, we revealed a positive correlation between TSPO levels in the mPFC and PPI scores, suggesting that a downregulation of prefrontal TSPO is associated with more severe sensorimotor gating impairments in animals with neurodevelopmental abnormalities. The precise relationship between prefrontal TSPO downregulation and sensorimotor gating impairments remains to be determined, but is in agreement with the known role of the mPFC in regulating sensorimotor gating and other neurocognitive processes.[95–98] The correlation between prefrontal TSPO and PPI in the MIA model is in line with a recent second-generation TSPO PET imaging study, indicating that lower TSPO binding in gray matter is associated with more severe psychopathology (as assessed using the Positive and Negative Syndrome Scale) and worse neurocognitive performance (as assessed using the Repeatable Battery for the Assessment of Neuropsychological Status) in untreated first-episode psychosis patients.[42] Interestingly, however, there was no correlation between inflammation-mediated impairments in social interaction and prefrontal TSPO levels, suggesting that the downregulation of prefrontal TSPO may be relevant only for a subset of schizophrenia-related behavioral dysfunctions.

Based on the findings obtained in the MIA model, our PET study focused on TSPO ligand binding in the MFG, which spans a substantial part of the human dorsolateral prefrontal cortex[71,72] and is structurally and functionally related to the mPFC in rodents.[73,74] Some early studies using the first-generation radiotracer [^{11}C]PK11195 found increased TSPO binding in temporal regions of patients with schizophrenia relative to CONs.[36,37] A number of more recent investigations, however, failed to replicate these findings, including studies using more selective second-generation TSPO radiotracers.[39–43] Importantly, a lack of increased (or even trends towards reduced) TSPO binding has been noted across various brain regions in antipsychotic naive, first-episode psychosis patients,[42,43] as well as in recent-onset schizophrenia patients with confirmed inflammatory cytokine alterations.[41] The current hypothesis-driven TSPO PET imaging approach, which focused specifically on the MFG of patients with recent-onset schizophrenia, is consistent with these latter studies. One limitation of the present study is that *in vivo* PET imaging was performed using one single TSPO radiotracer only. To this end, we selected the second-generation radiotracer [^{11}C]DPA-713, which shows an increased signal-to-noise ratio as compared with the prototypical first-generation radiotracer [^{11}C]PK11195.[44,45,68] As various second-generation TSPO ligands are currently available,[44] our study cannot be considered comprehensive with respect to comparing multiple second-generation radiotracers. However, distinct second-generation TSPO radiotracers are largely identical in terms of their binding specificity and pharmacokinetics,[26,99,100] so that we would expect similar findings when using other second-generation TSPO ligands.

Thus far, only one study reported increased TSPO ligand binding using a second-generation radiotracer in patients with schizophrenia or subjects at ultra-high risk of psychosis.[38] In this study, Bloomfield *et al.*[38] found a small ($< 5\%$) but significant increase in TSPO binding ratios in total gray matter as well as in temporal and frontal lobes of affected individuals relative to matched CONs. This positive report, however, was not based on analysis of regional distribution volumes (V_T), but rather relied on distribution volume ratios as the primary outcome measure. The latter approach may complicate interpretations for PET radiotracer studies involving TSPO, which lack a true reference region.[75,101]

Interestingly, the direct comparison between *ex vivo* autoradiography and immunohistochemical techniques in the MIA model revealed inconsistent results with regards to prefrontal TSPO expression and binding. Whereas a TSPO downregulation was confirmed in two independent cohorts of MIA offspring using immunohistochemistry, *ex vivo* autoradiography with first- or second-generation TSPO ligands did not reveal such differences. Several previous studies assessed the extent to which *ex vivo* TSPO autoradiography correlates with *in vivo* PET imaging using first-generation ([^{11}C]PK11195) and second-generation (including [^{11}C]DPA-713) TSPO radiotracers in excitotoxicity- or autoimmune-induced models of severe neuroinflammation.[102–104] These within-species studies revealed clear correlations between the *ex vivo* and *in vivo* approaches, at least when measured in the pathological context of severe reactive gliosis.[102–104] Given these correlations, we believe that the inconsistent findings obtained by TSPO immunohistochemistry and autoradiography in the MIA model are readily explainable by the lower resolution of *ex vivo* radiotracer assays as compared with immunohistochemical techniques, the latter of which can provide analyses at the cellular and subcellular resolution level.[105] Therefore, the latter technique is likely to be more suitable for detecting relatively small changes in TSPO expression in small organs such as the mouse brain,

whereas *in vivo* TSPO PET imaging may still yield satisfactory results in larger organs such the human brain.

In conclusion, our study has a number of implications for current attempts to define neuroimmune profiles in schizophrenia and related disorders using the TSPO biomarker. First, reduced TSPO expression can occur concomitantly with signs of central low-grade inflammation. Hence, decreased TSPO expression does not (necessarily) suggest reduced inflammation (and vice versa), implying furthermore that ongoing inflammatory processes are not always mirrored by increased TSPO signals. Without the concomitant assessment of additional inflammatory markers such as cytokines, interpreting 'neuroinflammation' on the sole basis of TSPO signals can readily lead to wrong conclusions. Second, altered TSPO levels do not reflect selective changes in microglia activity, neither in (infection-mediated) neurodevelopmental pathologies nor in severe neuroinflammatory conditions that are accompanied by marked microgliosis. Our study thus underscores the need to interpret *in vivo* or *ex vivo* imaging signals using TSPO radiotracers with caution, especially when such readouts are not complemented with other measures of inflammatory processes. Unless more selective glial markers are available for PET imaging, quantification of cytokines and other inflammatory biomarkers, along with their molecular signaling pathways,[4,8–12,14–16,41] may not only be more sensitive, but also more accurate, in attempts to characterize inflammatory profiles in schizophrenia and other mental disorders that lack robust reactive gliosis.

CONFLICT OF INTEREST

ACV has previously received grant support from F. Hoffmann-La Roche Ltd. The remaining authors declare no conflict of interest. The present work is purely academic.

ACKNOWLEDGMENTS

We thank Professor Jean-Marc Fritschy (Institute of Pharmacology and Toxicology, University of Zurich, Switzerland) for his technical assistance in the immunohistochemical procedures. We are also thankful to Dr Sandra Giovanoli for her assistance in behavioral experimentation and stereological analyses. This work was supported by the Swiss National Science Foundation (grant nos 310030_146217 and 310030_169544) and the Foundation for Research in Science and the Humanities at the University of Zurich awarded to UM. Additional financial support for this study was provided by NARSAD (awarded to JC and AS), the Alexander Wilson Schweizer Fellowship (awarded to JC), by a Silvio O. Conte Center grant (MH094268, awarded to AS) and by the Medical Research Council (New Investigator Grant, MR/N025377/1, awarded to ACV).

AUTHOR CONTRIBUTIONS

Study concept and design: TN, JMC, AS and UM. Generation of animal models: TN, UW and TG. Acquisition of animal data: TN, UW and DB. Analysis and interpretation of animal data: TN, UW, ACV, DB and UM. Acquisition of human data: JMC, YW, MGP and AS. Analysis and interpretation of human data: JMC, TN, YW, MGP, MK, AS and UM. Drafting of the manuscript: TN and UM. Critical revision of the manuscript for important intellectual content: TN, JMC, TG, UW, YW, KM, ACV, DB, MGP, AS and UM.

REFERENCES

1 Owen MJ, Sawa A, Mortensen PB. Schizophrenia. *Lancet* 2016; **388**: 86–97.
2 Kirkpatrick B, Miller BJ. Inflammation and schizophrenia. *Schizophr Bull* 2013; **39**: 1174–1179.
3 Khandaker GM, Cousins L, Deakin J, Lennox BR, Yolken R, Jones PB. Inflammation and immunity in schizophrenia: implications for pathophysiology and treatment. *Lancet Psychiatry* 2015; **2**: 258–270.
4 Landek-Salgado MA, Faust TE, Sawa A. Molecular substrates of schizophrenia: homeostatic signaling to connectivity. *Mol Psychiatry* 2016; **21**: 10–28.
5 Brown AS, Derkits EJ. Prenatal infection and schizophrenia: a review of epidemiologic and translational studies. *Am J Psychiatry* 2010; **167**: 261–280.
6 Meyer U. Developmental neuroinflammation and schizophrenia. *Prog Neuropsychopharmacol Biol Psychiatry* 2013; **42**: 20–34.
7 Potvin S, Stip E, Sepehry AA, Gendron A, Bah R, Kouassi E. Inflammatory cytokine alterations in schizophrenia: a systematic quantitative review. *Biol Psychiatry* 2008; **63**: 801–808.
8 Goldsmith DR, Rapaport MH, Miller BJ. A meta-analysis of blood cytokine network alterations in psychiatric patients: comparisons between schizophrenia, bipolar disorder and depression. *Mol Psychiatry* 2016; **21**: 1696–1709.
9 Hayes LN, Severance EG, Leek JT, Gressitt KL, Rohleder C, Coughlin JM *et al.* Inflammatory molecular signature associated with infectious agents in psychosis. *Schizophr Bull* 2014; **40**: 963–972.
10 Volk DW, Chitrapu A, Edelson JR, Roman KM, Moroco AE, Lewis DA. Molecular mechanisms and timing of cortical immune activation in schizophrenia. *Am J Psychiatry* 2015; **172**: 1112–1121.
11 Fillman SG, Cloonan N, Catts VS, Miller LC, Wong J, McCrossin T *et al.* Increased inflammatory markers identified in the dorsolateral prefrontal cortex of individuals with schizophrenia. *Mol Psychiatry* 2013; **18**: 206–214.
12 Trépanier MO, Hopperton KE, Mizrahi R, Mechawar N, Bazinet RP. Postmortem evidence of cerebral inflammation in schizophrenia: a systematic review. *Mol Psychiatry* 2016; **21**: 1009–1026.
13 Bernstein HG, Steiner J, Guest PC, Dobrowolny H, Bogerts B. Glial cells as key players in schizophrenia pathology: recent insights and concepts of therapy. *Schizophr Res* 2015; **161**: 4–18.
14 Fillman SG, Sinclair D, Fung SJ, Webster MJ, Shannon Weickert C. Markers of inflammation and stress distinguish subsets of individuals with schizophrenia and bipolar disorder. *Transl Psychiatry* 2014; **4**: e365.
15 Fillman SG, Weickert TW, Lenroot RK, Catts SV, Bruggemann JM, Catts VS *et al.* Elevated peripheral cytokines characterize a subgroup of people with schizophrenia displaying poor verbal fluency and reduced Broca's area volume. *Mol Psychiatry* 2016; **21**: 1090–1098.
16 Miller BJ, Buckley P, Seabolt W, Mellor A, Kirkpatrick B. Meta-analysis of cytokine alterations in schizophrenia: clinical status and antipsychotic effects. *Biol Psychiatry* 2011; **70**: 663–671.
17 Mondelli V, Ciufolini S, Belvederi Murri M, Bonaccorso S, Di Forti M, Giordano A *et al.* Cortisol and inflammatory biomarkers predict poor treatment response in first episode psychosis. *Schizophr Bull* 2015; **41**: 1162–1170.
18 Müller N, Riedel M, Scheppach C, Brandstätter B, Sokullu S, Krampe K *et al.* Beneficial antipsychotic effects of celecoxib add-on therapy compared to risperidone alone in schizophrenia. *Am J Psychiatry* 2002; **159**: 1029–1034.
19 Meyer U, Schwarz MJ, Müller N. Inflammatory processes in schizophrenia: a promising neuroimmunological target for the treatment of negative/cognitive symptoms and beyond. *Pharmacol Ther* 2011; **132**: 96–110.
20 Keller WR, Kum LM, Wehring HJ, Koola MM, Buchanan RW, Kelly DL. A review of anti-inflammatory agents for symptoms of schizophrenia. *J Psychopharmacol* 2013; **27**: 337–342.
21 Sommer IE, van Westrhenen R, Begemann MJ, de Witte LD, Leucht S, Kahn RS. Efficacy of anti-inflammatory agents to improve symptoms in patients with schizophrenia: an update. *Schizophr Bull* 2014; **40**: 181–191.
22 Pasternak O, Kubicki M, Shenton ME. *In vivo* imaging of neuroinflammation in schizophrenia. *Schizophr Res* 2016; **173**: 200–212.
23 Watkins CC, Andrews SR. Clinical studies of neuroinflammatory mechanisms in schizophrenia. *Schizophr Res* 2016; **176**: 14–22.
24 Owen DR, Matthews PM. Imaging brain microglial activation using positron emission tomography and translocator protein-specific radioligands. *Int Rev Neurobiol* 2011; **101**: 19–39.
25 Turkheimer FE, Rizzo G, Bloomfield PS, Howes O, Zanotti-Fregonara P, Bertoldo A *et al.* The methodology of TSPO imaging with positron emission tomography. *Biochem Soc Trans* 2015; **43**: 586–592.
26 Vivash L, O'Brien TJ. Imaging microglial activation with TSPO PET: lighting up neurologic diseases? *J Nucl Med* 2016; **57**: 165–168.
27 Venneti S, Lopresti BJ, Wiley CA. The peripheral benzodiazepine receptor (Translocator protein 18kDa) in microglia: from pathology to imaging. *Prog Neurobiol* 2006; **80**: 308–322.
28 Papadopoulos V, Baraldi M, Guilarte TR, Knudsen TB, Lacapère JJ, Lindemann P *et al.* Translocator protein (18kDa): new nomenclature for the peripheral-type benzodiazepine receptor based on its structure and molecular function. *Trends Pharmacol Sci* 2006; **27**: 402–409.
29 Rupprecht R, Papadopoulos V, Rammes G, Baghai TC, Fan J, Akula N *et al.* Translocator protein (18 kDa) (TSPO) as a therapeutic target for neurological and psychiatric disorders. *Nat Rev Drug Discov* 2010; **9**: 971–988.
30 Gut P, Zweckstetter M, Banati RB. Lost in translocation: the functions of the 18-kD translocator protein. *Trends Endocrinol Metab* 2015; **26**: 349–356.
31 Sandiego CM, Gallezot JD, Pittman B, Nabulsi N, Lim K, Lin SF *et al.* Imaging robust microglial activation after lipopolysaccharide administration in humans with PET. *Proc Natl Acad Sci USA* 2015; **112**: 12468–12473.

32 Hannestad J, Gallezot JD, Schafbauer T, Lim K, Kloczynski T, Morris ED *et al.* Endotoxin-induced systemic inflammation activates microglia: [^{11}C]PBR28 positron emission tomography in nonhuman primates. *Neuroimage* 2012; **63**: 232–239.
33 Papadopoulos V, Lecanu L. Translocator protein (18 kDa) TSPO: an emerging therapeutic target in neurotrauma. *Exp Neurol* 2009; **219**: 53–57.
34 Kreisl WC, Lyoo CH, Liow JS, Wei M, Snow J, Page E *et al.* (11)C-PBR28 binding to translocator protein increases with progression of Alzheimer's disease. *Neurobiol Aging* 2016; **44**: 53–61.
35 Janssen B, Vugts DJ, Funke U, Molenaar GT, Kruijer PS, van Berckel BN *et al.* Imaging of neuroinflammation in Alzheimer's disease, multiple sclerosis and stroke: Recent developments in positron emission tomography. *Biochim Biophys Acta* 2016; **1862**: 425–441.
36 van Berckel BN, Bossong MG, Boellaard R, Kloet R, Schuitemaker A, Caspers E *et al.* Microglia activation in recent-onset schizophrenia: a quantitative (R)-[11C] PK11195 positron emission tomography study. *Biol Psychiatry* 2008; **64**: 820–822.
37 Doorduin J, de Vries EF, Willemsen AT, de Groot JC, Dierckx RA, Klein HC. Neuroinflammation in schizophrenia-related psychosis: a PET study. *J Nucl Med* 2009; **50**: 1801–1807.
38 Bloomfield PS, Selvaraj S, Veronese M, Rizzo G, Bertoldo A, Owen DR *et al.* Microglial activity in people at ultra high risk of psychosis and in schizophrenia: An [(11)C]PBR28 PET brain imaging study. *Am J Psychiatry* 2016; **173**: 44–52.
39 Kenk M, Selvanathan T, Rao N, Suridjan I, Rusjan P, Remington G *et al.* Imaging neuroinflammation in gray and white matter in schizophrenia: an in-vivo PET study with [18 F]-FEPPA. *Schizophr Bull* 2015; **41**: 85–93.
40 Takano A, Arakawa R, Ito H, Tateno A, Takahashi H, Matsumoto R *et al.* Peripheral benzodiazepine receptors in patients with chronic schizophrenia: a PET study with [11C]DAA1106. *Int J Neuropsychopharmacol* 2010; **13**: 943–950.
41 Coughlin JM, Wang Y, Ambinder EB, Ward RE, Minn I, Vranesic M *et al. In vivo* markers of inflammatory response in recent-onset schizophrenia: a combined study using [(11)C]DPA-713 PET and analysis of CSF and plasma. *Transl Psychiatry* 2016; **6**: e777.
42 Hafizi S, Tseng HH, Rao N, Selvanathan T, Kenk M, Bazinet RP *et al.* Imaging microglial activation in untreated first-episode psychosis: A PET study with [^{18}F] FEPPA. *Am J Psychiatry*; e-pub ahead of print 9 September 2016; doi: appiajp201616020171.
43 Holmes SE, Hinz R, Drake RJ, Gregory CJ, Conen S, Matthews JC *et al. In vivo* imaging of brain microglial activity in antipsychotic-free and medicated schizophrenia: a [11C](R)-PK11195 positron emission tomography study. *Mol Psychiatry* 2016; **21**: 1672–1679.
44 Chauveau F, Boutin H, Van Camp N, Dollé F, Tavitian B. Nuclear imaging of neuroinflammation: a comprehensive review of [11C]PK11195 challengers. *Eur J Nucl Med Mol Imaging* 2008; **35**: 2304–2319.
45 Endres CJ, Pomper MG, James M, Uzuner O, Hammoud DA, Watkins CC *et al.* Initial evaluation of 11C-DPA-713, a novel TSPO PET ligand, in humans. *J Nucl Med* 2009; **50**: 1276–1282.
46 Meyer U, Feldon J. Epidemiology-driven neurodevelopmental animal models of schizophrenia. *Prog Neurobiol* 2010; **90**: 285–326.
47 Meyer U. Prenatal poly(I:C) exposure and other developmental immune activation models in rodent systems. *Biol Psychiatry* 2014; **75**: 307–315.
48 Meyer U, Feldon J, Fatemi SH. In-vivo rodent models for the experimental investigation of prenatal immune activation effects in neurodevelopmental brain disorders. *Neurosci Biobehav Rev* 2009; **33**: 1061–1079.
49 Reisinger S, Khan D, Kong E, Berger A, Pollak A, Pollak DD. The poly(I:C)-induced maternal immune activation model in preclinical neuropsychiatric drug discovery. *Pharmacol Ther* 2015; **149**: 213–226.
50 Meyer U, Feldon J, Schedlowski M, Yee BK. Towards an immuno-precipitated neurodevelopmental animal model of schizophrenia. *Neurosci Biobehav Rev* 2005; **29**: 913–947.
51 Garay PA, Hsiao EY, Patterson PH, McAllister AK. Maternal immune activation causes age- and region-specific changes in brain cytokines in offspring throughout development. *Brain Behav Immun* 2013; **31**: 54–68.
52 Giovanoli S, Weber-Stadlbauer U, Schedlowski M, Meyer U, Engler H. Prenatal immune activation causes hippocampal synaptic deficits in the absence of overt microglia anomalies. *Brain Behav Immun* 2016; **55**: 25–38.
53 Lévesque M, Avoli M. The kainic acid model of temporal lobe epilepsy. *Neurosci Biobehav Rev* 2013; **37**: 2887–2899.
54 Zattoni M, Mura ML, Deprez F, Schwendener RA, Engelhardt B, Frei K *et al.* Brain infiltration of leukocytes contributes to the pathophysiology of temporal lobe epilepsy. *J Neurosci* 2011; **31**: 4037–4050.
55 Vezzani A, Conti M, De Luigi A, Ravizza T, Moneta D, Marchesi F *et al.* Interleukin-1beta immunoreactivity and microglia are enhanced in the rat hippocampus by focal kainate application: functional evidence for enhancement of electrographic seizures. *J Neurosci* 1999; **19**: 5054–5065.
56 De Simoni MG, Perego C, Ravizza T, Moneta D, Conti M, Marchesi F *et al.* Inflammatory cytokines and related genes are induced in the rat hippocampus by limbic status epilepticus. *Eur J Neurosci* 2000; **12**: 2623–2633.
57 Pernot F, Heinrich C, Barbier L, Peinnequin A, Carpentier P, Dhote F *et al.* Inflammatory changes during epileptogenesis and spontaneous seizures in a mouse model of mesiotemporal lobe epilepsy. *Epilepsia* 2011; **52**: 2315–2325.
58 Braff DL, Geyer MA, Swerdlow NR. Human studies of prepulse inhibition of startle: normal subjects, patient groups, and pharmacological studies. *Psychopharmacology* 2001; **156**: 234–258.
59 Dodell-Feder D, Tully LM, Hooker CI. Social impairment in schizophrenia: new approaches for treating a persistent problem. *Curr Opin Psychiatry* 2015; **28**: 236–242.
60 Crawley JN. Translational animal models of autism and neurodevelopmental disorders. *Dialogues Clin Neurosci* 2012; **14**: 293–305.
61 Vuillermot S, Weber L, Feldon J, Meyer U. A longitudinal examination of the neurodevelopmental impact of prenatal immune activation in mice reveals primary defects in dopaminergic development relevant to schizophrenia. *J Neurosci* 2010; **30**: 1270–1287.
62 Weber-Stadlbauer U, Richetto J, Labouesse MA, Bohacek J, Mansuy IM, Meyer U. Transgenerational transmission and modification of pathological traits induced by prenatal immune activation. *Mol Psychiatryt*; e-pub ahead of print 29 March 2016; doi: 10.1038/mp.2016.41.
63 Notter T, Panzanelli P, Pfister S, Mircsof D, Fritschy JM. A protocol for concurrent high-quality immunohistochemical and biochemical analyses in adult mouse central nervous system. *Eur J Neurosci* 2014; **39**: 165–175.
64 Selemon LD, Zecevic N. Schizophrenia: a tale of two critical periods for prefrontal cortical development. *Transl Psychiatry* 2015; **5**: e623.
65 Tamminga CA, Stan AD, Wagner AD. The hippocampal formation in schizophrenia. *Am J Psychiatry* 2010; **167**: 1178–1193.
66 Ralvenius WT, Benke D, Acuña MA, Rudolph U, Zeilhofer HU. Analgesia and unwanted benzodiazepine effects in point-mutated mice expressing only one benzodiazepine-sensitive GABAA receptor subtype. *Nat Commun* 2015; **6**: 6803.
67 Burguillos MA. Use of meso-scale discovery™ to examine cytokine content in microglia cell supernatant. *Methods Mol Biol* 2013; **1041**: 93–100.
68 Kim T, Pae AN. Translocator protein (TSPO) ligands for the diagnosis or treatment of neurodegenerative diseases: a patent review (2010-2015; part 1). *Expert Opin Ther Pat* 2016; **13**: 1–27.
69 Owen DR, Gunn RN, Rabiner EA, Bennacef I, Fujita M, Kreisl WC *et al.* Mixed-affinity binding in humans with 18-kDa translocator protein ligands. *J Nucl Med* 2011; **52**: 24–32.
70 Owen DR, Yeo AJ, Gunn RN, Song K, Wadsworth G, Lewis A *et al.* An 18-kDa translocator protein (TSPO) polymorphism explains differences in binding affinity of the PET radioligand PBR28. *J Cereb Blood Flow Metab* 2012; **32**: 1–5.
71 Petrides M, Pandya DN. Dorsolateral prefrontal cortex: comparative cytoarchitectonic analysis in the human and the macaque brain and corticocortical connection patterns. *Eur J Neurosci* 1999; **11**: 1011–1036.
72 Kikinis Z, Fallon JH, Niznikiewicz M, Nestor P, Davidson C, Bobrow L *et al.* Gray matter volume reduction in rostral middle frontal gyrus in patients with chronic schizophrenia. *Schizophr Res* 2010; **123**: 153–159.
73 Uylings HB, Groenewegen HJ, Kolb B. Do rats have a prefrontal cortex? *Behav Brain Res* 2003; **146**: 3–17.
74 Seamans JK, Lapish CC, Durstewitz D. Comparing the prefrontal cortex of rats and primates: insights from electrophysiology. *Neurotox Res* 2008; **14**: 249–262.
75 Innis RB, Cunningham VJ, Delforge J, Fujita M, Gjedde A, Gunn RN *et al.* Consensus nomenclature for in vivo imaging of reversibly binding radioligands. *J Cereb Blood Flow Metab* 2007; **27**: 1533–1539.
76 Malkova NV, Yu CZ, Hsiao EY, Moore MJ, Patterson PH. Maternal immune activation yields offspring displaying mouse versions of the three core symptoms of autism. *Brain Behav Immun* 2012; **26**: 607–616.
77 Schwartzer JJ, Careaga M, Onore CE, Rushakoff JA, Berman RF, Ashwood P. Maternal immune activation and strain specific interactions in the development of autism-like behaviors in mice. *Transl Psychiatry* 2013; **3**: e240.
78 Kreisl WC, Jenko KJ, Hines CS, Lyoo CH, Corona W, Morse CL *et al.* A genetic polymorphism for translocator protein 18 kDa affects both in vitro and in vivo radioligand binding in human brain to this putative biomarker of neuroinflammation. *J Cereb Blood Flow Metab* 2013; **33**: 53–58.
79 Cosenza-Nashat M, Zhao ML, Suh HS, Morgan J, Natividad R, Morgello S *et al.* Expression of the translocator protein of 18 kDa by microglia, macrophages and astrocytes based on immunohistochemical localization in abnormal human brain. *Neuropathol Appl Neurobiol* 2009; **35**: 306–328.
80 Ji B, Maeda J, Sawada M, Ono M, Okauchi T, Inaji M *et al.* Imaging of peripheral benzodiazepine receptor expression as biomarkers of detrimental versus beneficial glial responses in mouse models of Alzheimer's and other CNS pathologies. *J Neurosci* 2008; **28**: 12255–12267.

81 Bae KR, Shim HJ, Balu D, Kim SR, Yu SW. Translocator protein 18 kDa negatively regulates inflammation in microglia. *J Neuroimmune Pharmacol* 2014; **9**: 424–437.
82 Ma L, Zhang H, Liu N, Wang PQ, Guo WZ, Fu Q *et al.* TSPO ligand PK11195 alleviates neuroinflammation and beta-amyloid generation induced by systemic LPS administration. *Brain Res Bull* 2016; **121**: 192–200.
83 Zhang H, Ma L, Yin YL, Dong LQ, Cheng GG, Ma YQ *et al.* Over-expression of TSPO in the hippocampal CA1 area alleviates cognitive dysfunction caused by lipopolysaccharide in mice. *Brain Res* 2016; **1646**: 402–409.
84 Daugherty DJ, Selvaraj V, Chechneva OV, Liu XB, Pleasure DE, Deng W. A TSPO ligand is protective in a mouse model of multiple sclerosis. *EMBO Mol Med* 2013; **5**: 891–903.
85 Ravikumar B, Crawford D, Dellovade T, Savinainen A, Graham D, Liere P *et al.* Differential efficacy of the TSPO ligands etifoxine and XBD-173 in two rodent models of multiple sclerosis. *Neuropharmacology* 2016; **108**: 229–237.
86 Gut P. Targeting mitochondrial energy metabolism with TSPO ligands. *Biochem Soc Trans* 2015; **43**: 537–542.
87 Morin D, Musman J, Pons S, Berdeaux A, Ghaleb B. Mitochondrial translocator protein (TSPO): From physiology to cardioprotection. *Biochem Pharmacol* 2016; **105**: 1–13.
88 Batoko H, Veljanovski V, Jurkiewicz P. Enigmatic translocator protein (TSPO) and cellular stress regulation. *Trends Biochem Sci* 2015; **40**: 497–503.
89 Banati RB, Middleton RJ, Chan R, Hatty CR, Kam WW, Quin C *et al.* Positron emission tomography and functional characterization of a complete PBR/TSPO knockout. *Nat Commun* 2014; **5**: 5452.
90 Coughlin JM, Ishizuka K, Kano SI, Edwards JA, Seifuddin FT, Shimano MA *et al.* Marked reduction of soluble superoxide dismutase-1 (SOD1) in cerebrospinal fluid of patients with recent-onset schizophrenia. *Mol Psychiatry* 2013; **18**: 10–11.
91 Steullet P, Cabungcal JH, Monin A, Dwir D, O'Donnell P, Cuenod M *et al.* Redox dysregulation, neuroinflammation, and NMDA receptor hypofunction: A "central hub" in schizophrenia pathophysiology? *Schizophr Res* 2016; **176**: 41–51.
92 Kulak A, Steullet P, Cabungcal JH, Werge T, Ingason A, Cuenod M *et al.* Redox dysregulation in the pathophysiology of schizophrenia and bipolar disorder: insights from animal models. *Antioxid Redox Signal* 2013; **18**: 1428–1443.
93 Cabungcal JH, Counotte DS, Lewis EM, Tejeda HA, Piantadosi P, Pollock C *et al.* Juvenile antioxidant treatment prevents adult deficits in a developmental model of schizophrenia. *Neuron* 2014; **83**: 1073–1084.
94 Oskvig DB, Elkahloun AG, Johnson KR, Phillips TM, Herkenham M. Maternal immune activation by LPS selectively alters specific gene expression profiles of interneuron migration and oxidative stress in the fetus without triggering a fetal immune response. *Brain Behav Immun* 2012; **26**: 623–634.
95 Bubser M, Koch M. Prepulse inhibition of the acoustic startle response of rats is reduced by 6-hydroxydopamine lesions of the medial prefrontal cortex. *Psychopharmacology* 1994; **113**: 487–492.
96 Japha K, Koch M. Picrotoxin in the medial prefrontal cortex impairs sensorimotor gating in rats: reversal by haloperidol. *Psychopharmacology* 1999; **144**: 347–354.
97 Yee BK. Cytotoxic lesion of the medial prefrontal cortex abolishes the partial reinforcement extinction effect, attenuates prepulse inhibition of the acoustic startle reflex and induces transient hyperlocomotion, while sparing spontaneous object recognition memory in the rat. *Neuroscience* 2000; **95**: 675–689.
98 Schwabe K, Koch M. Role of the medial prefrontal cortex in N-methyl-D-aspartate receptor antagonist induced sensorimotor gating deficit in rats. *Neurosci Lett* 2004; **355**: 5–8.
99 Oh U, Fujita M, Ikonomidou VN, Evangelou IE, Matsuura E, Harberts E *et al.* Translocator protein PET imaging for glial activation in multiple sclerosis. *J Neuroimmune Pharmacol* 2011; **6**: 354–361.
100 Colasanti A, Guo Q, Muhlert N, Giannetti P, Onega M, Newbould RD *et al. In vivo* assessment of brain white matter inflammation in multiple sclerosis with 18 F-PBR111 PET. *J Nucl Med* 2014; **55**: 1112–1118.
101 Narendran R, Frankle WG. Comment on analyses and conclusions of "Microglial Activity in people at ultra high risk of psychosis and in schizophrenia: an [(11)C] PBR28 PET brain imaging study". *Am J Psychiatry* 2016; **173**: 536–537.
102 Boutin H, Chauveau F, Thominiaux C, Grégoire MC, James ML, Trebossen R *et al.* 11C DPA-713: a novel peripheral benzodiazepine receptor PET ligand for *in vivo* imaging of neuroinflammation. *J Nucl Med* 2007; **48**: 573–581.
103 Chauveau F, Van Camp N, Doll´e F, Kuhnast B, Hinnen F, Damont A *et al.* Comparative evaluation of the translocator protein radioligands 11C-DPA-713, 18 F-DPA-714, and 11C-PK11195 in a rat model of acute neuroinflammation. *J Nucl Med* 2009; **50**: 468–476.
104 Xie L, Yamasaki T, Ichimaru N, Yui J, Kawamura K, Kumata K *et al.* [11C]DAC-PET for noninvasively monitoring neuroinflammation and immunosuppressive therapy efficacy in rat experimental autoimmune encephalomyelitis model. *J Neuroimmune Pharmacol* 2012; **7**: 231–242.
105 Miyashita T. Confocal microscopy for intracellular co-localization of proteins. *Methods Mol Biol* 2015; **1278**: 515–526.

Supplementary Information accompanies the paper on the Molecular Psychiatry website (http://www.nature.com/mp)